

# Event Transformer<sup>+</sup>. A multi-purpose solution for efficient event data processing

Alberto Sabater, Luis Montesano, and Ana C. Murillo

arXiv:2211.12222v1 [cs.CV] 22 Nov 2022

**Abstract**—Event cameras record sparse illumination changes with high temporal resolution and high dynamic range. Thanks to their sparse recording and low consumption, they are increasingly used in applications such as AR/VR and autonomous driving. Current top-performing methods often ignore specific event-data properties, leading to the development of generic but computationally expensive algorithms, while event-aware methods do not perform as well. We propose *Event Transformer<sup>+</sup>*, that improves our seminal work *EvT* with a refined patch-based event representation and a more robust backbone to achieve more accurate results, while still benefiting from event-data sparsity to increase its efficiency. Additionally, we show how our system can work with different data modalities and propose specific output heads, for event-stream predictions (i.e. action recognition) and per-pixel predictions (dense depth estimation). Evaluation results show better performance to the state-of-the-art while requiring minimal computation resources, both on GPU and CPU.

## 1 INTRODUCTION

Event cameras register changes in intensity at each pixel of the sensor array providing, with minimal power consumption, asynchronous sparse information with an increased High Dynamic Range and a high temporal resolution (in the order of microseconds). Many applications such as AR/VR or autonomous driving can take advantage of this type of cameras, especially when computational power is limited or when dealing with challenging motion and lightning conditions. Although this type of sensors are relatively recent, they have already shown good results in action recognition [5], [15], tracking [6], [29], depth estimation [10], [42] or odometry [18], [28]. The most common way to process event streams converts them into frame representations and use state of the art algorithms based on Convolutional Neural Networks [1], [3], [7], [15] and/or Recurrent Layers [7], [15]. These frame-like representations ignore the natural sparsity of event cameras. There are also methods that try to exploit this sparsity and, consequently, are more efficient, e.g. PointNet-like Neural Networks [41], Graph Neural Networks [5], [8] or Spike Neural Networks [17], [33]. However, they usually obtain lower accuracy.

This paper proposes Event Transformer<sup>+</sup>, a novel solution (overview in Fig. 1) for efficient event data processing without sacrificing performance. It extends our previous

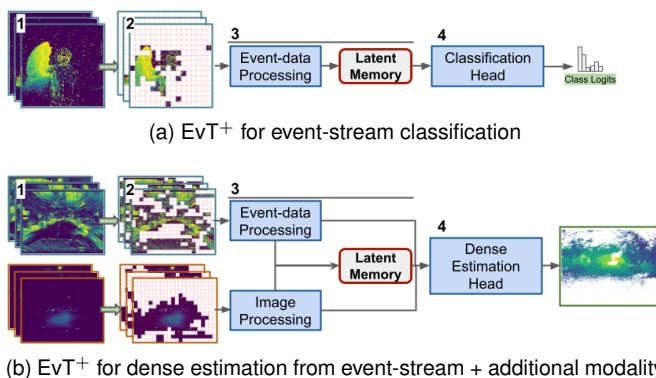


Fig. 1. **Framework overview.** Areas (*activated patches* (2)) from the input data (event frame-representations and images, (1)) with sufficient information are extracted and processed by the EvT<sup>+</sup> *backbone* (3) to update a set of *latent memory* vectors. Different output heads (4) are used for: a) event-stream classification by processing the latent memory, and b) multi-modal dense estimation by updating and further processing the input information with the latent memory vectors.

work on Event Transformer [30] in three ways. First, we use a finer patch-based event data representation with richer spatio-temporal information, while still benefiting from its sparsity. Second, it improves the Event Transformer backbone with a more robust data processing, which we adapt to jointly use information from different data modalities (e.g., event data and grayscale images). In addition to this, we also show how Event Transformer<sup>+</sup> can be combined with different output heads to perform either event-stream predictions, i.e., classification, or per-pixel predictions, i.e. dense estimation.

We have evaluated the new EvT<sup>+</sup> in two different tasks with real event data benchmarks. First, we evaluated it for event-stream classification, in particular gesture recognition, where it improves prior work performance, including our previous EvT solution. Second, we evaluated it for dense per-pixel estimation tasks, in particular dense depth estimation. This latter task also includes the use of multi-modal inputs, in particular events and grayscale images. In all cases, our validation demonstrates that EvT<sup>+</sup> obtains better results than the state-of-the-art for the different tasks, while performing very efficiently.

- A. Sabater, L. Montesano, and A.C. Murillo are with DIIS-I3A, Universidad de Zaragoza, Spain
- L. Montesano is also with Bitbrain Technologies, Spain.

## 2 RELATED WORK

This section summarizes the most common approaches for event data representation as well as event-based Neural Network architectures that process them. It also includes a brief summary of available event-based datasets.

### 2.1 Event data representation

Event data representations encode the event information related to a time-interval or temporal-window extracted from an event-stream. These representations can be divided in two categories: **event-level representations** usually treat the event data as graphs [4], [5], [8], [41] or point-clouds [31], [38] with minimal pre-processing and keeping the event data sparsity; differently, **frame-based representations** group incoming events into dense frame-like arrays, ignoring the event data sparsity but easing a later learning process. Our work is built on the top of frame-based representations, where we find plenty of variations in the literature. The *time-surfaces* [19] build frames encoding the last generated event for each pixel. SP-LSTM [24] builds frames where each pixel contains a value related to the existence of an event in a time-window and its polarity. The *Surfaces of Active Events* [22] builds frames where each pixel contains a measurement of the time between the last observed event and the beginning of the accumulation time. *Motion-compensated* [27], [39] generate frames by aligning events according to the camera ego-motion. [11] binarizes frame representations in the temporal dimension, achieving a better time-resolution. TBR [15] aggregates binarized frame representations into single-bins frames. M-LSTM [7] uses a grid of LSTMs that processes incoming events at each pixel to create a final 2D representation. TORE [3] uses FIFOs to retain the last events for each pixel. EvT [30] build histogram-like representations for each pixel and divide the frame representation into patches, ignoring the ones with not enough event information.

The present work build patch representations like EvT, but from a refined frame representation, based on the use of FIFOs to retain events distributed sparsely on time. The proposed hybrid solution presents benefits from both the event-level representations, since we can to a certain extent tackle the sparsity of the event data, but also from the robustness of the frame-based representations.

### 2.2 Neural Network architectures for event data

**Event-stream classification** has been addressed in different ways in the literature. First, we find some efficient architectures that process sparse event representations such as Spike Neural Networks [17], [33], [44], PointNet-style Networks [41] or Graph neural Networks [4], [5], [8]. Most common, other rely on CNNs to process event-frame representations [1], [3], [7], [15]. For long event-stream processing, they are split into shorter time-windows that are frequently processed independently, and then aggregated with Recurrent Networks [15], [43], CNNs [1], [15], temporal buffers [3], [8], or voting between the intermediate results [15].

Depending on the aggregation strategy, we consider that an event-processing algorithm is able to perform **online inference** if it can evaluate the information within each

time-window incrementally, as it is generated, and then perform the final visual recognition with minimal latency, as opposed to the processing of all the captured information in a large batch. Our approach performs online inference by updating incrementally a set of latent memory vectors with simple addition operations, and processing the resulting vectors with a simple classifier.

When it comes to **event-stream dense estimation**, dense event representations and CNNs to process them are the most common scenario. LMDDE [12] uses fully convolutional networks to process the event-data and ConvLSTMs to handle their temporality. ULODE [48] trains a CNN to deblur event representations and predict optical flow, egomotion and depth. ECN [45] uses an Evenly-Cascaded Convolutional Network to predict optical flow, egomotion and depth. DTL [40] use CNNs to translate events to images for semantic segmentation and depth estimation. RAM-Net [10] uses CNNs to encode both grayscale and event frames and ConvGRUs to update a hidden state with the temporal information, used later to perform multi-modal depth estimation. LMDDE [12] and RAM-Net [10] propose synthetic datasets to be used as pre-training.

Differently, we complement our sparse tokens (already processed by our backbone) with dummy tokens to create a dense representation that is then updated with the information from our latent memory vectors. Then, similar to RGB solutions, [26] we use skip connections between the self-attention blocks in the encoder and the dense output head to generate the final dense output.

### 2.3 Event dataset recordings

Large-scale public datasets recorded with event cameras in real scenarios are scarce. This lack has motivated many works to propose different approaches to translate RGB datasets to their event-based counterpart. Earlier approaches [5], [13], [20], [25], [32] display RGB data in a LCD monitor and then record the display with an event-camera. More recent approaches introduce the use of learning-based emulators [9], [14], [23] to generate event data. Unfortunately, these translated datasets cannot fully mimic the event-data nature and introduce certain artifacts, specially on their sparsity and latency. In order to have a more reliable evaluation setup, we focus our experimentation on datasets recorded with event-cameras on real scenarios. More specifically, we train and evaluate EvT<sup>+</sup> for event-stream classification [1], [35], and multi-modal dense estimation [47].

## 3 EVENT TRANSFORMER FRAMEWORK

Different to traditional RGB cameras, event cameras log the captured visual information in a sparse and asynchronous manner. Each time the event camera detects an intensity change, it triggers an event  $e = \{x, y, t, p\}$  defined by its location  $(x, y)$  within the sensor grid  $(H \times W)$ , its timestamp  $t$  (in the order of  $\mu s$ ) and its polarity  $p$  (either positive or negative change). In the following, we detail the EvT<sup>+</sup> contributions in terms of event-data representation and processing for classification and dense estimation tasks.

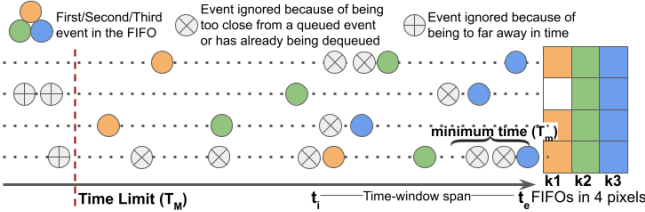
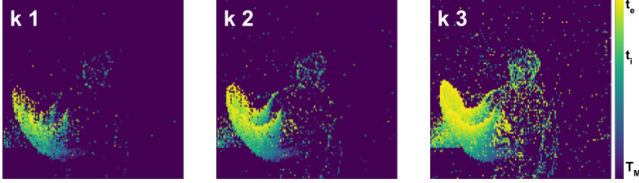
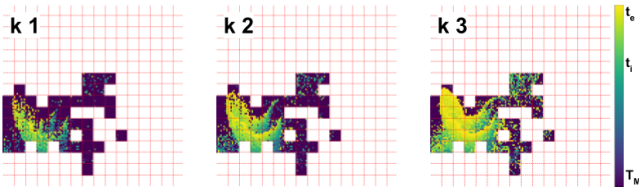
(a) Event accumulation using FIFOs of size  $K = 3$ (b) Sample frame-like representation for different values of  $K$ (c) Activated patches for different values of  $K$ 

Fig. 2. Patch-based event data representation. (a) For each pixel we retain the last  $K$  events taking into account sufficient sparsity in time. (b) Frame-like representations are built with the time-stamps of the queued events. (c) Frame representations are split into patches, keeping only the activated patches, i.e., with enough event information.

### 3.1 Patch-based event data representation

Similarly to previous work [1], [3], [5], [15], [30], [41], we create a frame representation for each time-window  $\Delta t$  that covers a time-span from  $t_i$  to  $t_e$ . Like TORE [3], we model this event information with queues  $FIFO(x, y, p, k)$  (see Fig. 2a) that retain  $k \in K$  events for each pixel ( $y \in H, x \in W$ ) within the sensor array and polarity ( $p \in \{0, 1\}$ ). But differently, for each pixel we do not retain the last  $K$  events but the last  $K$  events that are separated by at least a minimum time of  $T_m = \frac{\Delta t}{K}$ . This threshold is intended to avoid the over-representation of the information provided by the events that happen consecutively in time. And additionally, when no events are registered in this time-window span for a certain pixel, we account for the ones triggered up to a maximum time  $T_M$  ( $T_M \gg \Delta t$  and  $T_M \ll t_i$ ).

Once the events are queued for a given time-window, we build an intermediate frame representation  $F^{H \times W \times K \times 2}$  with their time-stamps (see Fig. 2b). We normalize the pixels to have a value in the range from 0 to  $T_M$  and then to scale their values to a 0 – 1 range (Eq. 1):

$$F = F - (t_e - T_M), F = F/T_M \quad (1)$$

Therefore, the events queued at the end of the time-window will have values close to 1 and the ones close to  $T_M$  will have a value close to 0.

Then, similar to EvT, we split the generated frame-representations into non-overlapping patches of size  $P \times P$  (see Fig. 2c), and we set each patch as *activated* if it contains a minimum  $m$  percent of pixels that have information of events triggered between  $t_i$  and  $t_e$ . Note that events trig-

gered between  $T_M$  and  $t_i$  are not involved in the patch activation decision, since they have been considered in previous time-windows, but they complement the patch information to ease later their processing. Activated patches are finally flattened to create tokens  $T$  of size  $(P^2 \cdot K \cdot 2)$ , input of the transformer backbone detailed in the next subsection.

### 3.2 Event Transformer

Transformers [37] are a natural way to process the patch-based representation we propose. Different to other architectures, they are able to ingest lists of tokens of variable length and process them with attention mechanisms. The later, different to convolutions, focus on the whole input data (structuring it as a Query ( $Q$ ), Key ( $K$ ) and Value ( $V$ )) to capture both local and long-range token dependencies:

$$Attention(Q, K, V) = softmax\left(\frac{QK^T}{\sqrt{d_k}}\right)V. \quad (2)$$

The processing core of our work, Event Transformer<sup>+</sup> (EvT<sup>+</sup>), is motivated by these ideas. As the patches  $T$  (whose length varies on their sparsity, as described in Section 3.1) from new time-windows are being generated, they are processed by this backbone with attention mechanisms. This process ends with the update of a set of  $M$  latent vectors. These vectors act as a memory that logs the key information seen so far and its final processing allows to perform tasks such as event-stream classification or dense per-pixel estimations. This whole process (detailed in Figure 3) is divided in the following steps:

- 1. Patch pre-processing** Each one of the  $T$  input activated patches is mapped to a vector of dimensionality  $D$ , constant along all the network. This transformation ( $FF1$ ) consists of an initial Feed Forward layer (FF), the concatenation of 2D-aware positional embeddings, and a last FF layer. The use of positional embeddings to augment the patch information is required since Transformers, unlike CNNs, cannot implicitly know the locality of the input data. An initial set of  $N_1$  Self-Attention blocks is then used to analyze long and short-range spatial dependencies between tokens. In the case of *multi-modal data processing*, a different patch pre-processing branch is used for each data modality (as summarized in Fig. 1b).

- 2. Backbone processing.** This backbone uses the pre-processed token information (as  $K - V$ ) to process the latent memory vectors  $M$  (as  $Q$ ) with a single Cross-Attention Module. The resulting  $M'$  vectors are then refined with  $N_2$  Self-Attention layers.

- 3. Memory update.** The latent memory vectors  $M$  are updated given the new generated vectors  $M'$  with a simple sum operation and normalization:

$$M = \|M + M'\| \quad (3)$$

This augmented version of the latent vectors encodes longer spatio-temporal information and is used to perform the final downstream task, for which we have implemented the following two options.

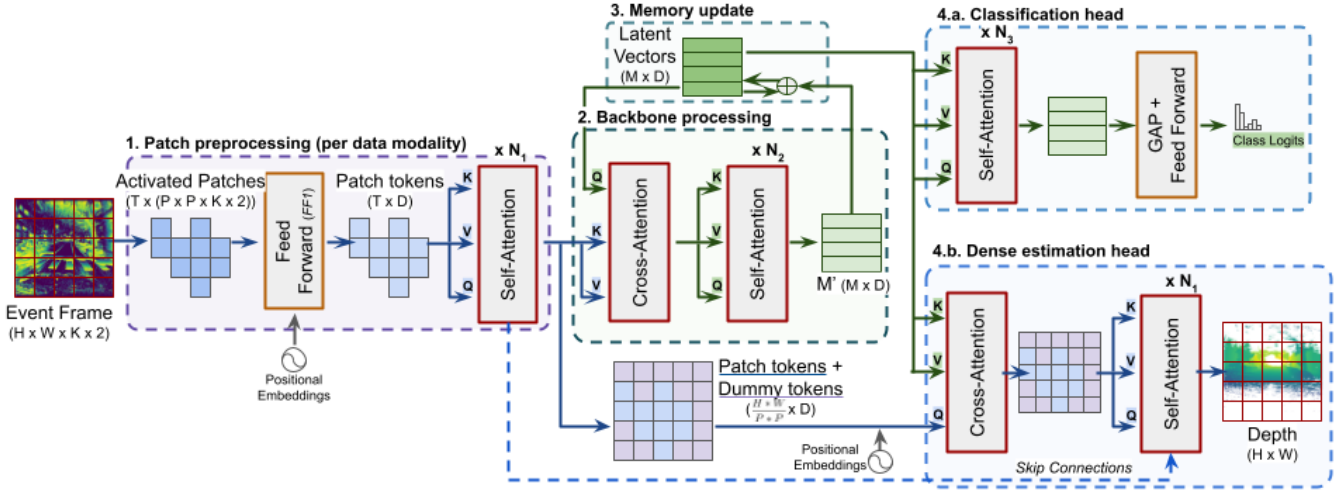


Fig. 3. Event Transformer<sup>+</sup> (EvT<sup>+</sup>) overview. The set of patch tokens  $T$  related to the events within a time-window (or any other data modality such as images) are processed to update a set of latent memory vectors. The later accumulate the seen information and are used to perform the final downstream task, i.e., in our framework event-stream classification or dense per-pixel estimation.

**4.a. Classification head.** Event-stream classification is performed by processing the refined latent memory vectors, that contain the key spatio-temporal information of the event-stream seen so far. This processing consists of  $N_3$  Self-Attention modules and then, similar to EvT, processing the resulting vectors with two Feed Forward layers and Global Average Pooling (GAP).

**4.b. Dense estimation head.** Given the sparse set of tokens processed at step 1 and their initial location in the input frame-representation, we convert them back to a dense representation by adding dummy tokens (initialized with zeroes) that complement the ones lost due to the event-data sparsity. We then add positional embedding information to this dense representation, and update it with the information contained in the latent memory vectors (used as  $Q-V$ ) with a Cross-Attention layer. The resulting final set of tokens is then refined with  $N_1$  Self-Attention layers, which have skip-connections from the  $N_1$  Self-Attention layers of the patch pre-processing step.

In the case of *multi-modal data processing*, the skip connections propagate the information jointly for each data modality, whose tokens are merged with a simple addition and normalization operation.

**Attention modules.** All the Cross and Self-Attention modules from EvT<sup>+</sup> share the same architecture, similar to previous transformer related works [2], [16], [30], [37], composed of a Multi-Head Attention layer [37], normalization layers, skip connections and Feed Forward layers.

### 3.3 Optimization

EvT<sup>+</sup> is optimized differently for different downstream tasks. In the case of **event-stream classification**, EvT<sup>+</sup> is optimized with the Negative Log-Likelihood loss:

$$\mathcal{L}_{NLL} = - \sum_i^n (Y_i \log \hat{Y}_i + (1 - Y_i) \log (1 - \hat{Y}_i)) \quad (4)$$

between the predicted labels  $\hat{Y}_i$  and the groundtruth labels  $Y_i$ , and label smoothing [46] for regularization.

In the case of **monocular dense estimation**, we train EvT<sup>+</sup> in the sparse depth labels measured by a LiDAR sensor. These ground-truth depth maps, similar to other methods [10], [12], are clipped to a range  $[D_m - D_M]$  captured by the sensor ( $[2 - 80]$  in our case of MVSEC Dataset) and we train EvT<sup>+</sup> to predict its normalized log depth representation  $\hat{Y} \in [0 - 1]$ :

$$\bar{Y} = \frac{\log(Y) - \log(D_m)}{\log(D_M) - \log(D_m)}. \quad (5)$$

We optimize EvT<sup>+</sup> as in [10] with a scale invariant loss

$$\mathcal{L}_{si} = \frac{1}{n} \sum_i^n (R_i)^2 - \frac{1}{n^2} \left( \sum_i^n R_i \right)^2, \quad (6)$$

and a multi-scale invariant loss

$$\mathcal{L}_{msi} = \frac{1}{n} \sum_k^4 \sum_i^n (|\nabla_x R_i^k| + |\nabla_y R_i^k|), \quad (7)$$

where  $n$  are the valid depth ground-truth points,  $R_i$  is the log-depth difference map  $\|\bar{Y}_i - \hat{Y}_i\|$  at the point  $i$ ,  $R_i^k$  is the log-depth difference map at the scale  $k \in [0 - 4]$ . Both losses are combined as  $\mathcal{L} = \mathcal{L}_{si} + \lambda \mathcal{L}_{msi}$ , with  $\lambda = 0.25$ .

## 4 EXPERIMENTS

This section includes the implementation and training details of the proposed Event Transformer<sup>+</sup> (EvT<sup>+</sup>) along with its experimental validation. We evaluate EvT<sup>+</sup> in two tasks (event-stream classification and monocular depth estimation), analyze its efficiency, and justify the EvT<sup>+</sup> design choices with a thorough ablation study.

### 4.1 Implementation and training details

**Patch-based event representation:** We set a patch size of  $10 \times 10$  for event-stream classification and  $12 \times 12$  for the depth estimation task, that has larger frame representations. In all cases the number of events in the FIFO,  $K$ , is set to 3,  $M_T$  is set to 256 ms, and the threshold  $m$  for the patch activation is set as in EvT (7.5%). Dataset-specific hyperparameters are discussed in the following Section 4.2.

**Event Transformer:** The latent vectors and the vector dimensionality  $D$  is set to 160. The latent memory is composed of 32 latent vectors. The positional encodings are initialized with 6 bands of 2D Fourier Features [34] ( $\frac{H}{P} \times \frac{W}{P} \times 24$ , being  $H$  and  $W$  the specific sensor height and width from each dataset). Both the latent vectors and positional encodings are learned as the rest of the parameters of the network during training. The amount of Attention layers  $N_1$ ,  $N_2$  and  $N_3$  are set to 1, but in the case of depth estimation,  $N_1$  is set to 2. All the Multi-Head Attention layers use 8 heads, but in the case of depth estimation that has bigger input size, we use only 4 in the pre-processing and decoding steps to increase their efficiency.

**Training details:** The whole framework is optimized with the AdamW optimizer [21] in a single NVIDIA Tesla V100, with the learning rate set to  $1e-3$  and using gradient clipping. The batch-size is 128 for event-stream classification and 24 for depth estimation. Data augmentation used consists of spatial and temporal random cropping, dropout, drop token, and repetition of each sample within the training batch twice with different augmentations.

## 4.2 Evaluation

The proposed Event Transformer<sup>+</sup> (EvT<sup>+</sup>) is evaluated in two scenarios of real event-camera recordings that represent different use cases. First, we evaluate EvT<sup>+</sup> to classify event-streams of human actions and gestures. Second, we demonstrate that our solution is also suitable for dense inference from a sparse input, in particular, using multi-modal (grayscale image and event data) dense depth estimation. Finally, we provide a detailed analysis on how EvT<sup>+</sup> takes advantage from the event-data sparsity to increase its efficiency, performing inferences with minimal latency.

### 4.2.1 Event-stream classification

EvT<sup>+</sup> is evaluated in two benchmarks for event-stream classification. The **DVS128 Gesture Dataset** [1] is composed of 1342 event-streams capturing 10 different human gestures (plus an optional extra category for random movements) and recorded with 29 different subjects under three different illumination conditions. The **SL-Animals-DVS Dataset** [35] is composed of 1121 event-streams capturing 19 different sign language gestures, executed by 58 different subjects, under different illumination conditions. Recordings from these two datasets last between 1 and 6 seconds and contain continuous repetitions of shorter human gestures. As detailed in Section 4.3, these recordings are cropped to up to 1298 and 1792 ms that are split into time-windows  $\Delta t$  of 24 and 48 ms for the DVS128 and SL-Animals-DVS datasets respectively.

Table 1 shows the accuracy of top-performing models in the DVS128 Dataset, with and without including the extra additional distractor class of random movements (11 and 10 classes respectively). The column *Online* highlights the ability of each model to perform online inference, i.e., incremental processing of the event data and classification with low latency. Similarly, Table 2 shows the accuracy of top-performing methods evaluated on the SL-Animals-DVS Dataset, a more demanding benchmark with lower state-of-the-art accuracy. 3 *Sets* results exclude the samples recorded

Model	10 Classes	11 Classes	Online
RG-CNN [5]	N/A	97.2	x
3D-CNN + Voting [15]	<b>99.58</b>	<b>99.62</b>	x
CNN [1]	96.49	94.59	✓
Space-time clouds [41]	97.08	95.32	✓
CNN + LSTM [15]	97.5	97.53	✓
TORE [3]	N/A	96.2	✓
EvT	98.46	96.20	✓
<b>EvT<sup>+</sup> (Ours)</b>	<b>99.24</b>	<b>97.57</b>	✓

TABLE 1  
Classification Accuracy in DVS128 Gesture Dataset. N/A = Not Available at the source reference

Model	3 Sets	4 Sets
SLAYER [36]	78.03	60.09
STBP [36]	71.45	56.20
DECOLLE [17]	77.6	70.6
TORE [3]	N/A	85.1
EvT	87.45	88.12
<b>EvT<sup>+</sup> (Ours)</b>	<b>92.34</b>	<b>94.39</b>

TABLE 2  
Classification Accuracy in SL-Animals-DVS. N/A = Not Available at the source reference

indoor with artificial lighting from a neon light source, since they include noise related to the reflection of clothing and the flickering of the fluorescent lamps. 4 *Sets* evaluates all the samples within the dataset.

Results from Table 1 show how our approach obtains better results than prior works, improving EvT in both data set-ups. Only [15] is more accurate than EvT<sup>+</sup> but it uses offline inference and 3D-CNNs, which are computationally expensive but have a good inductive bias, useful when training with small datasets like DVS128 and with random movements (as it is the case of 11 Classes). As for the more challenging SL-Animals Dataset, EvT<sup>+</sup> achieves a new state-of-the-art, outperforming prior methods by a large margin. Interestingly, our solution presents higher robustness to the different lightning conditions of the 4 *Sets*, being able to take advantage of larger training set to achieve better accuracy.

### 4.2.2 Monocular multi-modal dense depth estimation

To evaluate EvT<sup>+</sup> for dense depth estimation we use the MVSEC Dataset [47]. This dataset includes stereo auto-movilistic recordings with event-data, grayscale images and depth maps captured by a LiDAR, captured by day (2 recordings) and at night (3 recordings). Similar to previous work, we use the *outdoor\_day\_2* sequence for training and the remaining 4 sequences for testing. Due to the corruption of different sequences, we limit the training and validation to the data recorded from the left sensors. Depth maps are always recorded at 20 Hz, but grayscale images are recorded at 45 Hz by day and 10 Hz by night, therefore, they are not synced with the depth maps.

Although the recorded sequences are very long, due to computational restrictions, we just consider (both for training and validation) the 512 ms of information for the depth map estimation. The event information from these sequences is split in time-windows  $\Delta t$  of 50 ms that are synced with the depth maps, and is complemented with a grayscale image generated at least  $\Delta t/2$  ms away from the end of each time-window. Therefore, all time-steps contain



Model	Events	Images	outdoor day 1			outdoor night 1			outdoor night 2			outdoor night 3		
			10	20	30	10	20	30	10	20	30	10	20	30
ULODE [48]	✓	✗	2.72	3.84	4.40	3.13	4.02	4.89	2.19	3.15	3.92	2.86	4.46	5.05
LMDDE [12]	✓	✗	2.70	3.46	3.84	5.36	5.32	5.40	2.80	3.28	3.74	2.39	2.88	3.39
LMDDE [12]*	✓	✗	1.85	2.64	3.13	3.38	3.82	4.46	1.67	2.63	3.58	<b>1.42</b>	2.33	3.18
EvT <sup>+</sup> (Ours)	✓	✗	<b>1.30</b>	<b>1.93</b>	<b>2.33</b>	<b>1.58</b>	<b>2.31</b>	<b>2.93</b>	<b>1.53</b>	<b>2.25</b>	<b>2.91</b>	<b>1.42</b>	<b>2.17</b>	<b>2.79</b>
RAM Net [10]**	✓	✓	1.39	2.17	2.76	2.50	3.19	3.82	<b>1.21</b>	2.31	3.28	<b>1.01</b>	2.34	3.43
EvT <sup>+</sup> (Ours)	✓	✓	<b>1.27</b>	<b>1.94</b>	<b>2.37</b>	<b>1.48</b>	<b>2.09</b>	<b>2.84</b>	1.48	<b>2.13</b>	<b>2.92</b>	1.40	<b>2.05</b>	<b>2.79</b>

\* Pre-training on DENSE [12] dataset.

\*\* Pre-training on EventScape [10] dataset.

TABLE 3

Evaluation on the MVSEC Dataset. Average absolute depth error in meters (lower is better) at different cut-off depth distances in meters (10, 20, 30). First block shows models trained just on event data. Second block shows models trained jointly with event and image (grayscale) data.

event-data but might not contain grayscale image information. This issue is more frequent in the night sequences, where the grayscale image frequency is lower. When there is no grayscale information, only the event tokens update the memory and are used to the later dense depth estimation.

Table 3 shows the average depth error of different models at different cut-off depths, i.e. pixels whose groundtruth depth information is under the specified threshold (10, 20, or 30 meters). As observed, EvT<sup>+</sup> is able to largely outperform previous methods in most of the set-ups, with no specific pre-training. More importantly, when including image data EvT<sup>+</sup> improves its accuracy to achieve higher robustness even in the most challenging scenarios.

#### 4.2.3 Event sparsity and model efficiency analysis.

We now provide a deeper analysis of the computational cost of EvT<sup>+</sup> and how it benefits from the data sparsity. In the case of event-stream classification, different to EvT where the computational cost ( $O(|T| \times M)$ ) depends on the cross-attention layer, the computational cost of EvT<sup>+</sup> depends on the initial self-attention pre-processing ( $O(|T|^2)$ ), where  $|T|$  stands for the amount of activated patches and  $M$  for the amount of latent memory vectors. This means that, similar to EvT, the cost lowers as the input data is more sparse, but it is not bounded by  $M$ . Although this cost is theoretically higher, as observed in Table 4, different implementation improvements such as bigger patch sizes  $P$  and less latent vectors  $M$ , make EvT<sup>+</sup> even more efficient (FLOPs and latency) than EvT for event-stream classification.

In the case of depth estimation, the existence of a dense output head that does not work with sparse information increases the computational cost to  $O(\frac{H*W^2}{P*P})$  (details in Table 5). This higher cost and the use of a bigger sensor size that generates more activated patches, make EvT<sup>+</sup> to have a higher cost than for event-stream classification. Still, the rest of the Neural Network benefits from the data sparsity by suppressing non-activated patches. This is also true for the ones generated from grayscale images, when pixels are black, specially in the night sequences.

However, since our network is very shallow, in all cases the final latency of EvT<sup>+</sup> is minimal, being able to perform inference in a time-span significantly shorter than the time-window  $\Delta t$  processed, both in GPU and CPU.

### 4.3 Ablation study

This subsection analyzes the influence of key components in our framework for event-stream classification. This evaluation has been performed with both the DVS128 Gesture

(10 classes) and the SL-Animals-DVS (4 sets) datasets. It also discusses the hyperparameters that are key to achieve better results for monocular depth estimation. For this study we use the multimodal version of EvT<sup>+</sup>.

**Event representation hyperparameters:** The key components of our event representation are the patch size ( $P$ ) used to split the event frame representations, the number of events  $K$  queued for each FIFO and the maximum sequence length used to represent each event-stream sequence. As observed in Fig. 4b, a higher patch size reduces the floating point operations required to process a single time-window, but from some point it also reduces the model accuracy. Differently, a higher value of the parameter  $K$  (Fig. 4c), used to split the event information for a certain time-window, also increases the required FLOPs without a significant increment of the model accuracy. In both cases, we select, as observed in the Figures, the value that presents a good trade-off between computational cost and accuracy. Finally, we observe in Fig. 4a that, in general terms, the accuracy increases with the sequence length used to describe an event-stream. It is important to notice that this length converges to a maximum accuracy since the sequences found in the datasets are made out of the repetition of shorter action movements. Also, larger event-stream sequence lengths could not be tested because of GPU memory restrictions.

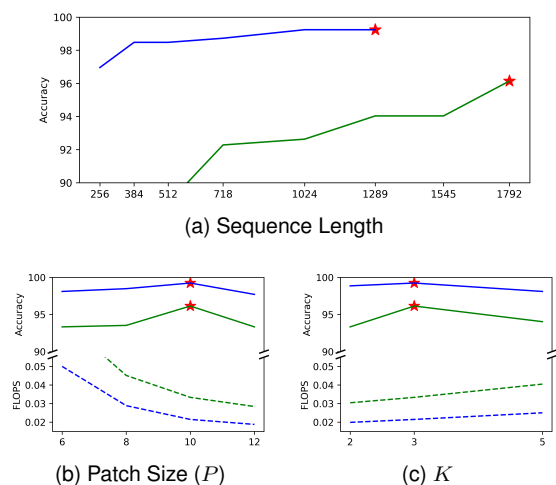


Fig. 4. EvT<sup>+</sup> accuracy with different data hyperparameters for the DVS128 Dataset - 10 classes (blue) and for the SL-Animals-Dataset - 4 Sets (green). Dashed lines: average FLOPs required to process a single time-window. Stars: the selected hyperparameter value.

**Backbone hyperparameters:** The most relevant backbone hyperparameter for the computational cost is the

Model	Sensor size	Dataset	T	$\Delta t$ ms	Latency (GPU/CPU)	FLOPs	#Params.
EvT	$128 \times 128$	SL-Animals	80	48	3 / 5 ms	0.09 G	0.48 M
EvT	$128 \times 128$	DVS128	45	24	2 / 4 ms	0.08 G	0.48 M
EvT <sup>+</sup>	$128 \times 128$	SL-Animals	32	48	2 / 4 ms	0.04 G	0.66 M
EvT <sup>+</sup>	$128 \times 128$	DVS128	18	24	3 / 3 ms	0.03 G	0.66 M
EvT <sup>+</sup>	$346 \times 260$	MVSEC	318	50	10 / 25 ms	2.94 G	1.98 M
EvT <sup>+</sup> (multi-modal)	$346 \times 260 \times 2$	MVSEC	318 + 319	50	15 / 37 ms	3.68 G	2.50 M

|T|: Amount of patch tokens  $\Delta t$ : time-window length where the activated patches are extracted from  
 GPU: NVIDIA GeForce RTX 2080 Ti CPU: Intel Core i7-9700K

TABLE 4

EvT<sup>+</sup> efficiency analysis: execution time and FLOPs per  $\Delta t$ . Average results for all validation samples in each dataset.

EvT <sup>+</sup> Step	FLOPs
Sparse token pre-processing	0.61
Backbone processing and Latent Vectors update	0.06
Dense output head	2.27

TABLE 5

Average FLOPs required to process a single time-window  $\Delta t$  and generate a dense output for depth estimation.

amount of self-attention layers applied over the input patch tokens. As observed in Fig. 5a, its use increases the model accuracy, but the application of many of these layers increases significantly the model complexity, without a benefit over its accuracy. This is probably due to an increase of the model instability during training. As observed in Fig. 5b, the use of self-attention after the cross-attention layers does not benefit EvT<sup>+</sup>, both in accuracy and model complexity. Differently, using self-attention in the classification decoder does help the classification accuracy with a minimal overhead. Finally, we note that different to EvT, using more latent vectors does not help the training accuracy.

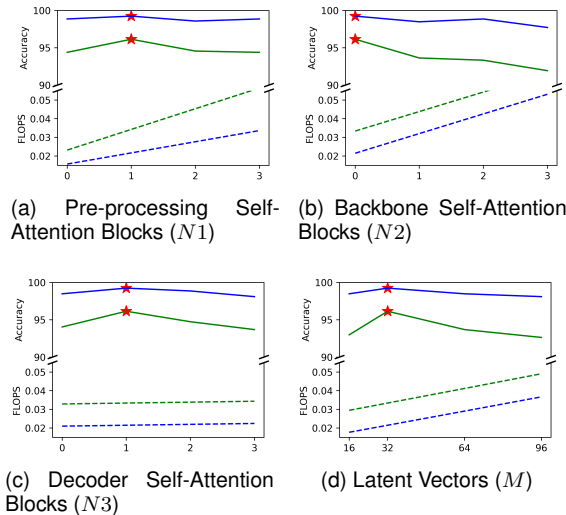


Fig. 5. EvT<sup>+</sup> accuracy with different model hyperparameters for the DVS128 Dataset - 10 classes (blue line) and for the SL-Animals-Dataset - 4 Sets (green line). Dashed lines: average FLOPs operations required. Stars: the selected hyperparameter value.

#### Backbone hyperparameters for dense estimation:

For multi-modal dense estimation where the sensor used to record the sequences have a bigger size, we find that increasing the patch size (Fig. 6a) not only reduces the FLOPs, but also increments the model performance (lower mean error).

Moreover, since this data presents higher complexity, we find that a more complex network is required to achieve better results. In particular, we find that the amount of pre-processing and backbone Self-Attention blocks (Fig. 6b and 6c) significantly affects the model performance, but at the cost of augmenting the computational requirements.

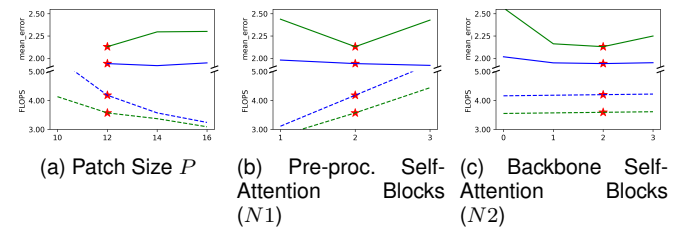


Fig. 6. EvT<sup>+</sup> average depth error at 20m crop rate and FLOPs on the *outdoor\_day\_1* (blue) and *outdoor\_night\_2* (green) sequences from MVSEC. Lower is better. Dashed lines: average amount FLOPs required to process a single time-window. Stars: selected hyperparameter value.

## 5 CONCLUSIONS

This work presents the Event Transformer<sup>+</sup> (EvT<sup>+</sup>) framework for event data processing, improving the seminal version of EvT. The proposed refined patch-based event representation and backbone compared to EvT are shown to provide more accurate results and increase further its efficiency for event-stream classification. This framework is demonstrated with a more complete validation, including the usage of data from different modalities and dense per pixel estimation tasks (in particular dense depth estimation) in addition to event-stream classification tasks. Evaluation results show better or comparable accuracy to the state-of-the-art while requiring significantly less computation resources, which makes EvT<sup>+</sup> able to work with minimal latency both on GPU and CPU. This work shows how patch-based representations and transformers are a promising line of research for efficient event-data processing and opens opportunities for further contributions with different kinds of sparse data such as LiDAR data.

## REFERENCES

- [1] Arnon Amir et al. A low power, fully event-based gesture recognition system. In *Proc. of the IEEE Conf. on Computer Vision and Pattern Recognition*, 2017.
- [2] Anurag Arnab, Mostafa Dehghani, Georg Heigold, Chen Sun, Mario Lučić, and Cordelia Schmid. Vivit: A video vision transformer. *arXiv preprint arXiv:2103.15691*, 2021.

- [3] Raymond Baldwin, Ruixu Liu, Mohammed Mutlaq Almatrafi, Vijayan K Asari, and Keigo Hirakawa. Time-ordered recent event (tore) volumes for event cameras. *IEEE Trans. on Pattern Analysis and Machine Intelligence*, 2022.
- [4] Yin Bi, Aaron Chadha, Alhabib Abbas, Eirina Bourtsoulatze, and Yiannis Andreopoulos. Graph-based object classification for neuromorphic vision sensing. In *Proc. of the IEEE/CVF Int. Conf. on Computer Vision*, 2019.
- [5] Yin Bi, Aaron Chadha, Alhabib Abbas, Eirina Bourtsoulatze, and Yiannis Andreopoulos. Graph-based spatio-temporal feature learning for neuromorphic vision sensing. *IEEE Trans. on Image Processing*, 2020.
- [6] Enrico Calabrese, Gemma Taverni, Christopher Awai Easthope, Sophie Sكريابine, Federico Corradi, Luca Longinotti, Kynan Eng, and Tobi Delbruck. Dhp19: Dynamic vision sensor 3d human pose dataset. In *Proc. of the IEEE/CVF Conf. on computer vision and pattern recognition workshops*, 2019.
- [7] Marco Cannici, Marco Ciccone, Andrea Romanoni, and Matteo Matteucci. A differentiable recurrent surface for asynchronous event-based data. In *European Conf. on Computer Vision*, 2020.
- [8] Yongjian Deng, Hao Chen, Huiying Chen, and Youfu Li. Evvgcn: A voxel graph cnn for event-based object classification. *arXiv preprint arXiv:2106.00216*, 2021.
- [9] Daniel Gehrig, Mathias Gehrig, Javier Hidalgo-Carrió, and Davide Scaramuzza. Video to events: Recycling video datasets for event cameras. In *Proc. of the IEEE/CVF Conf. on Computer Vision and Pattern Recognition*, 2020.
- [10] Daniel Gehrig, Michelle Rüegg, Mathias Gehrig, Javier Hidalgo-Carrió, and Davide Scaramuzza. Combining events and frames using recurrent asynchronous multimodal networks for monocular depth prediction. *IEEE Robotics and Automation Letters*, 2021.
- [11] Rohan Ghosh, Anupam Gupta, Andrei Nakagawa, Alcimar Soares, and Nitish Thakor. Spatiotemporal filtering for event-based action recognition. *arXiv preprint arXiv:1903.07067*, 2019.
- [12] Javier Hidalgo-Carrió, Daniel Gehrig, and Davide Scaramuzza. Learning monocular dense depth from events. In *2020 International Conference on 3D Vision (3DV)*. IEEE, 2020.
- [13] Yuhuang Hu, Hongjie Liu, Michael Pfeiffer, and Tobi Delbruck. Dvs benchmark datasets for object tracking, action recognition, and object recognition. *Frontiers in neuroscience*, 2016.
- [14] Yuhuang Hu, Shih-Chii Liu, and Tobi Delbruck. V2e: From video frames to realistic dvs events. In *Proc. of the IEEE/CVF Conf. on Computer Vision and Pattern Recognition*, 2021.
- [15] Simone Undri Innocenti, Federico Becattini, Federico Pernici, and Alberto Del Bimbo. Temporal binary representation for event-based action recognition. In *2020 25th International Conference on Pattern Recognition (ICPR)*. IEEE, 2021.
- [16] Andrew Jaegle, Felix Gimeno, Andrew Brock, Andrew Zisserman, Oriol Vinyals, and Joao Carreira. Perceiver: General perception with iterative attention. *arXiv preprint arXiv:2103.03206*, 2021.
- [17] Jacques Kaiser, Hesham Mostafa, and Emre Neftci. Synaptic plasticity dynamics for deep continuous local learning (decolle). *Frontiers in Neuroscience*, 2020.
- [18] Simon Klenk, Jason Chui, Nikolaus Demmel, and Daniel Cremers. Tum-vie: The tum stereo visual-inertial event dataset. *arXiv preprint arXiv:2108.07329*, 2021.
- [19] Xavier Lagorce, Garrick Orchard, Francesco Galluppi, Bertram E Shi, and Ryad B Benosman. Hots: a hierarchy of event-based time-surfaces for pattern recognition. *IEEE Trans. on pattern analysis and machine intelligence*, 2016.
- [20] Hongmin Li, Hanchao Liu, Xiangyang Ji, Guoqi Li, and Luping Shi. Cifar10-dvs: an event-stream dataset for object classification. *Frontiers in neuroscience*, 2017.
- [21] Ilya Loshchilov and Frank Hutter. Decoupled weight decay regularization. *arXiv preprint arXiv:1711.05101*, 2017.
- [22] Elias Mueggler, Christian Forster, Nathan Baumli, Guillermo Gallego, and Davide Scaramuzza. Lifetime estimation of events from dynamic vision sensors. In *2015 IEEE international conference on Robotics and Automation (ICRA)*. IEEE, 2015.
- [23] Jalees Nehvi, Vladislav Golyanik, Franziska Mueller, Hans-Peter Seidel, Mohamed Elgharib, and Christian Theobalt. Differentiable event stream simulator for non-rigid 3d tracking. In *Proc. of the IEEE/CVF Conf. on Computer Vision and Pattern Recognition*, 2021.
- [24] Anh Nguyen, Thanh-Toan Do, Darwin G Caldwell, and Nikos G Tsagarakis. Real-time 6dof pose relocalization for event cameras with stacked spatial lstm networks. In *Proc. of the IEEE/CVF Conf. on Computer Vision and Pattern Recognition Workshops*, 2019.
- [25] Garrick Orchard, Ajinkya Jayawant, Gregory K Cohen, and Nitish Thakor. Converting static image datasets to spiking neuromorphic datasets using saccades. *Frontiers in neuroscience*, 2015.
- [26] René Ranftl, Alexey Bochkovskiy, and Vladlen Koltun. Vision transformers for dense prediction. In *Proc. of the IEEE/CVF Int. Conf. on Computer Vision*, 2021.
- [27] Henri Rebecq, Timo Horstschaef, and Davide Scaramuzza. Real-time visual-inertial odometry for event cameras using keyframe-based nonlinear optimization. In *British Machine Vision Conference (BMVC)*, 2017.
- [28] Juan Pablo Rodríguez-Gómez, Raul Tapia, Julio L Paneque, Pedro Grau, Augusto Gómez Eguíluz, Jose Ramiro Martínez-de Dios, and Anibal Ollero. The griffin perception dataset: Bridging the gap between flapping-wing flight and robotic perception. *IEEE Robotics and Automation Letters*, 2021.
- [29] Viktor Rudnev, Vladislav Golyanik, Jiayi Wang, Hans-Peter Seidel, Mueller, et al. Eventhands: Real-time neural 3d hand pose estimation from an event stream. In *Proc. of the IEEE/CVF Int. Conf. on Computer Vision*, 2021.
- [30] Alberto Sabater, Luis Montesano, and Ana C. Murillo. Event transformer: a sparse-aware solution for efficient event data processing. In *Proc. of the IEEE/CVF Conf. on Computer Vision and Pattern Recognition Workshops*, June 2022.
- [31] Yusuke Sekikawa, Kosuke Hara, and Hideo Saito. Eventnet: Asynchronous recursive event processing. In *Proc. of the IEEE/CVF Conf. on Computer Vision and Pattern Recognition*, 2019.
- [32] Teresa Serrano-Gotarredona and Bernabé Linares-Barranco. A  $128 \times 1281.5\%$  contrast sensitivity  $0.9\%$  fpn  $3 \mu\text{s}$  latency  $4 \text{ mW}$  asynchronous frame-free dynamic vision sensor using transimpedance preamplifiers. *IEEE Journal of Solid-State Circuits*, 2013.
- [33] Sumit Bam Shrestha and Garrick Orchard. Slayer: Spike layer error reassignment in time. In *NeurIPS*, 2018.
- [34] Matthew Tancik et al. Fourier features let networks learn high frequency functions in low dimensional domains. *arXiv preprint arXiv:2006.10739*, 2020.
- [35] Ajay Vasudevan, Pablo Negri, Camila Di Ielsi, Bernabé Linares-Barranco, and Teresa Serrano-Gotarredona. SI-animals-dvs: event-driven sign language animals dataset. *Pattern Analysis and Applications*, 2021.
- [36] Ajay Vasudevan, Pablo Negri, Bernabé Linares-Barranco, and Teresa Serrano-Gotarredona. Introduction and analysis of an event-based sign language dataset. In *Int. Conf. on Automatic Face and Gesture Recognition*. IEEE, 2020.
- [37] Ashish Vaswani, Noam Shazeer, Niki Parmar, Jakob Uszkoreit, Llion Jones, Aidan N Gomez, Lukasz Kaiser, and Illia Polosukhin. Attention is all you need. In *Advances in neural information processing systems*, 2017.
- [38] Sai Vemprala, Sami Mian, and Ashish Kapoor. Representation learning for event-based visuomotor policies. *ArXiv*, abs/2103.00806, 2021.
- [39] Antoni Rosinol Vidal, Henri Rebecq, Timo Horstschaef, and Davide Scaramuzza. Ultimate slam? combining events, images, and imu for robust visual slam in hdr and high-speed scenarios. *IEEE Robotics and Automation Letters*, 2018.
- [40] Lin Wang, Yujeong Chae, and Kuk-Jin Yoon. Dual transfer learning for event-based end-task prediction via pluggable event to image translation. In *Proc. of the IEEE/CVF Int. Conf. on Computer Vision*, 2021.
- [41] Qinyi Wang, Yexin Zhang, Junsong Yuan, and Yilong Lu. Space-time event clouds for gesture recognition: From rgb cameras to event cameras. In *IEEE Winter Conf. on Applications of Computer Vision (WACV)*, 2019.
- [42] Ziwei Wang, Liyuan Pan, Yonhon Ng, Zheyu Zhuang, and Robert Mahony. Stereo hybrid event-frame (shef) cameras for 3d perception. In *IEEE/RSJ Int. Conf. on Intelligent Robots and Systems*, 2021.
- [43] Wenming Weng, Yueyi Zhang, and Zhiwei Xiong. Event-based video reconstruction using transformer. In *Proc. of the IEEE/CVF Int. Conf. on Computer Vision*, 2021.
- [44] Yujie Wu, Lei Deng, Guoqi Li, Jun Zhu, and Luping Shi. Spatio-temporal backpropagation for training high-performance spiking neural networks. *Frontiers in neuroscience*, 2018.
- [45] Chengxi Ye, Anton Mitrokhin, Cornelia Fermüller, James A Yorke, and Yiannis Aloimonos. Unsupervised learning of dense optical flow, depth and egomotion with event-based sensors. In *2020 IEEE/RSJ International Conference on Intelligent Robots and Systems (IROS)*. IEEE, 2020.
- [46] Chang-Bin Zhang, Peng-Tao Jiang, Qibin Hou, Yunchao Wei, Qi Han, Zhen Li, and Ming-Ming Cheng. Delving deep into label smoothing. *IEEE Trans. on Image Processing*.
- [47] Alex Zihao Zhu, Dinesh Thakur, Tolga Özaslan, Bernd Pfrommer, Vijay Kumar, and Kostas Daniilidis. The multivehicle stereo event camera dataset: An event camera dataset for 3d perception. *IEEE Robotics and Automation Letters*, 2018.



- [48] Alex Zihao Zhu, Liangzhe Yuan, Kenneth Chaney, and Kostas Daniilidis. Unsupervised event-based learning of optical flow, depth, and egomotion. In *Proc. of the IEEE/CVF Conf. on Computer Vision and Pattern Recognition*, 2019.